The Low-Mass X-ray Binary X1832−330
in the Globular Cluster NGC 6652:
A Serendipitous ASCA Observation

Koji Mukai[1] and Alan P. Smale[1]

Code 662, NASA/Goddard Space Flight Center, Greenbelt, MD 20771, USA.

ABSTRACT

The Low Mass X-ray Binary (LMXB) X1832−330 in NGC 6652 is one of 12 bright, or transient, X-ray sources to have been discovered in Globular Clusters. We report on a serendipitous *ASCA* observation of this Globular Cluster LMXB, during which a Type I burst was detected and the persistent, non-burst emission of the source was at its brightest level recorded to date. No orbital modulation was detected, which argues against a high inclination for the X1832−330 system. The spectrum of the persistent emission can be fit with a power law plus a partial covering absorber, although other models are not ruled out. Our time-resolved spectral analysis through the burst shows, for the first time, clear evidence for spectral cooling from kT=2.4±0.6 keV to kT=1.0±0.1 keV during the decay. The measured peak flux during the burst is ∼10% of the Eddington luminosity for a $1.4M_\odot$ neutron star. These are characteristic of a Type I burst, in the context of the relatively low quiescent luminosity of X1832−330.

Subject headings: X-ray: burst, stars

1.   Introduction

Of the ∼150 globular clusters associated with the Milky Way galaxy, 12 have been seen to harbor a bright ($L_x > 10^{36}$ ergs s^{-1}), or transient, low-mass X-ray binary (LMXB) (van Paradijs et al 1995). These binaries are presumably formed through stellar encounters in the dense cores of the clusters; such events play an important role in the dynamical evolution of the clusters, as the formation of a single LMXB can impart enough kinetic energy to the surrounding stars to terminate a core collapse. At the same time, the globular cluster LMXBs provide a unique opportunity to study LMXBs at a well-known distance with a well-known (and usually very poor) metalicity level.

---

[1]Also Universities Space Research Association

The X-ray source X1832−330 in the globular cluster NGC 6652 is a lesser known example of this class. Although the error box for the *HEAO-1* source, H1825−331, contained this cluster, it was originally not considered to be a secure identification because the error box covered a 2.7 deg^2 area in Sagittarius (Hertz & Wood 1985). The first secure detection of X1832−330 as a globular cluster LMXB was made during the course of the *ROSAT* all-sky survey (Predehl et al 1991). More recently, it was detected in pointed *ROSAT* observations (Johnston et al 1996), and two Type I X-ray bursts from this source, as well as the persistent emission, have been detected using the Wide Field Camera of the *BeppoSAX* satellite (in't Zand et al 1998). Thus there is now a strong circumstantial evidence that the *HEAO-1* source H1825−331 and X1832−330are the same source; here we have adopted this identification as a working assumption.

In the abovementioned papers, the distance to X1832−330 was assumed to be ∼14.3 kpc. However, the first published color-magnitude diagram of this cluster (Ortolani et al 1994) has led to the re-evaluation of the distance to ∼9.3 kpc, based on the measured V magnitudes V_{HB}=15.85±0.04 of its horizontal branch (as well as the interstellar reddening, $E_{(B-V)}$=0.10±0.02). Moreover, NGC 6652 appears to be significantly younger than the average globular clusters (Chaboyer et al 1996). Thus the LMXB X1832−330 in NGC 6652 may provide an important comparison with other globular cluster sources, due to the relative youth and the relatively high metal content ([Fe/H]=−0.96) of this cluster (though not the highest among globular clusters with LMXBs).

A search for the optical counterpart has recently been carried out using new ground-based data along with archival HST data (Deutsch et al 1998). Although the archival HST observations do not completely cover the X-ray error circle, the most promising candidate for the optical counterpart is their star 49, which is relatively faint (M_B=+5.5) compared with those of other globular cluster LMXBs.

In this paper, we present our analysis of a serendipitous *ASCA* observation of X1832−330; in comparing the previous observations with the *ASCA* data, we have recalculated the previously-published source luminosities for a new fiducial distance of 9.3 kpc.

2.   Observation

The region of the sky containing NGC 6652 was observed with the Japanese X-ray satellite, *ASCA* (Tanaka et al 1994) between 1996 Apr 6 20:12UT and Apr 7 19:00 UT (seq no 54016000). This observation was part of a program to observe diffuse Galactic emission, and only serendipitously included X1832−330 in its field of view. There are four co-aligned X-ray telescopes on-board *ASCA*, two with SIS (Solid-state Imaging Spectrometers, using CCDs) detectors and two with GIS (Gas Imaging Spectrometers) detectors. However, little useful data were taken with GIS-2, due to

a problem with its on-board processor[2].

No such problems exist for the SIS data; however, the observation was done with both SIS detectors in 4-CCD mode, with X1832−330 near the center of the field of view. This pointing direction minimizes the vignetting, but the photons from X1832−330 are spread over all 4 chips, complicating the analysis. Moreover, 4-CCD observations suffer most severely from the cumulative effect of radiation damage. As a consequence, events below ∼0.7 keV had to be discarded on-board to avoid telemetry saturation due to flickering pixels, and the spectral resolution and the quantum efficiency are both severely degraded (Dotani et al 1995). The degradation is believed to be due largely to residual dark distribution (RDD): a significant fractions of the CCD pixels now show elevated levels of dark current, the histogram of which is strongly skewed. When RDD-affected data are processed (on-board or on the ground) assuming a Gaussian distribution of dark current, this leads to incorrect pulse heights or spurious rejection of X-ray events as particle events. The current version of the response generator has a model of the degrading spectral resolution, but not one of the degrading quantum efficiency. We have used the FTOOL, `correctrdd`, which partially recovers the detection efficiency; however, this algorithm is not 100% effective. Moreover, the calibration of RDD-corrected data is uncertain. Therefore, we have primarily relied on the GIS data, cross-calibrated the RDD-corrected SIS data against the GIS data, and used the SIS data only when GIS data were unavailable.

Since a bright source is clearly detected (see below), we have opted to use loose sets of screening criteria. For the GIS, we use non-SAA, non-Earth-occult (ELV> 5°) data at the standard high-voltage setting, and only exclude regions where the cut-off rigidity is less than 4 GeV/c; note that, for safety reasons, the high voltage is reduced well before the satellite enters the SAA. After screening, we are left with ∼42 ksec of good GIS-3 data.

For the SIS, we use additional criteria that the line of sight must be >20° away from the sunlit Earth, the time after day/night and SAA transitions must be >128 s, and the PIXL monitor counts for the CCD chips must be within the 3σ of their mean value. Moreover, we have imposed the condition that the data must have been taken in the Faint mode. To correct for RDD and DFE (dark frame error, the variation in the mean dark level of all the pixels due primarily to scattered light on the CCD), we have applied `faintdfe` to the original Faint mode data first, followed by `correctrdd`, before converting to Bright2 mode, to minimize the interference between DFE and RDD corrections). This resulted in ∼21 ksec of good SIS data.

We have tested the calibration of RDD-corrected SIS data, by performing simultaneous fits to the GIS-3 and SIS data. We find that, even after the RDD correction, the best-fit SIS model contains a spurious excess N_H of 1.6×10^{21} cm^{-2} as well as a normalization below that of the GIS-3 data by a factor of 1.17.

---

[2]This problem had been noticed during the ground contact around 1996 Apr 5 20UT but initial attempt to fix this was unsuccessful. After the software was reloaded, the CPU returned to normal status at Apr 7 18:12UT. There is therefore ∼40 min of useful GIS-2 data, which we have chosen not to analyze.

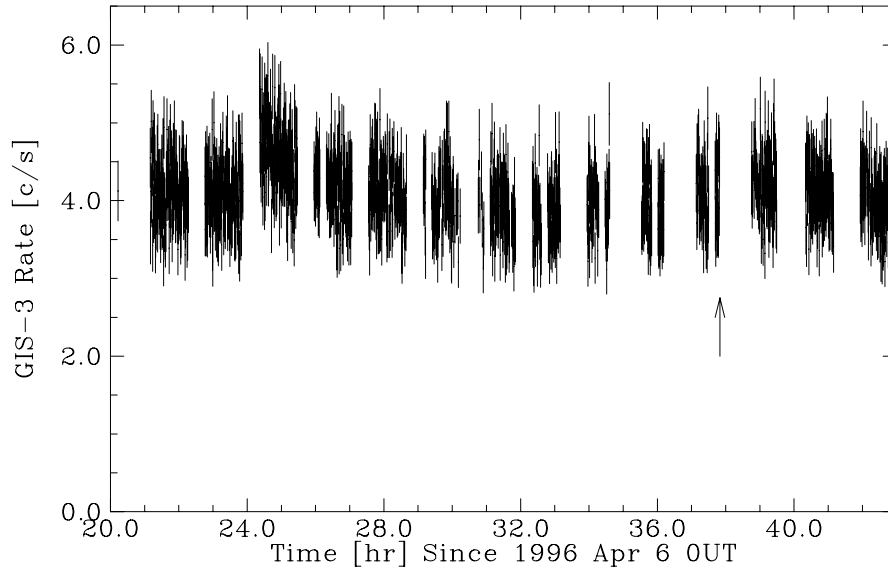## 3. Results

3.1. GIS-3 Data

Fig. 1.— The GIS-3 light curve of X1832−330, in 128 s bins. The arrow indicates the time of the burst, which occurred at the begging of a GIS-3 data gap.

In Fig.1, we have plotted the background subtracted light curve of X1832−330 in 128 s bins. The source appears variable on short timescales (from about a few bins of this diagram down to 4 sec): a straight line fit to a 4-s bin light curve, after removing the longer-term trend (by subtracting a 256-s running average of itself) yields a χ^2_ν of 1.114 for 10479 degrees of freedom, meaning that the source is variable at a formal confidence level of $1 - (1 \times 10^{-15})$. However, some caution is required at this level: although background is negligible, there may be systematic contribution to this apparent variability from, e.g., attitude jitter or the imperfect correction of the time-dependent detector gain. Moreover, a Fourier transform did not reveal a periodicity in the range 8 s to ∼1 hr (with an RMS amplitude of ∼0.5% in this range); the highest peaks in the periodogram in this range have semi-amplitudes of 1.6 %, while a signal would have to have an amplitude of >2 % to be detected at >99% confidence.

Although there are some possible peaks in the periodogram at longer periods, we consider these to be rather unreliable, since they can be explained as due to an interplay of the quasi-regular data gaps and the increased count rate between 0 and 2 UT on Apr 7 (see Fig. 1); this flare-like event may well be part of the aperiodic variability. We do not see spectral changes during this flare-like event (such as might be expected were it the tail of a Type I burst). The highest peaks in the periodogram are at P=46600s (>half the duration of the observation) with a 4.5% amplitude,

and at 17400 s (2.8%). Although non-sinusoidal modulation (e.g., dipping activities) with certain periods (e.g., near the 96 min spacecraft orbit) may have eluded detection, this would seem to require an unfortunate coincidence.
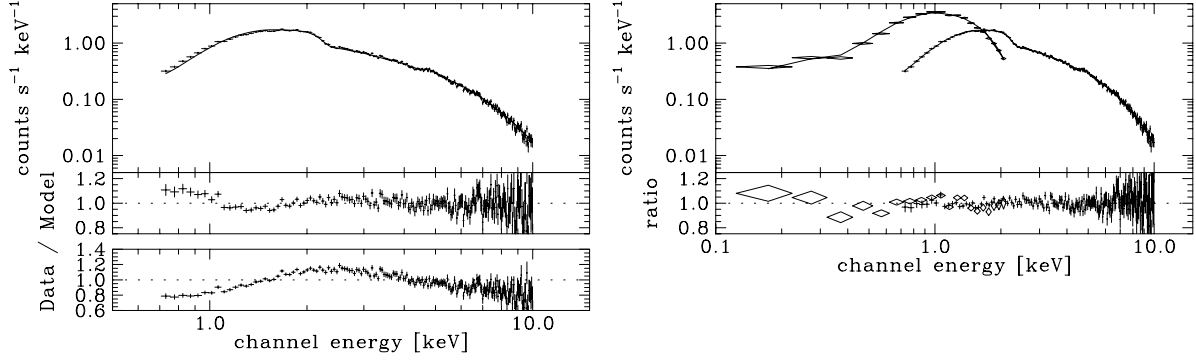

Fig. 2.— (a) The average GIS-3 spectrum of X1832−330, plotted with the best-fit power-law model (top), with the residuals shown in the form of the data/model ratio (middle). In the bottom panel, we show the residual for the best-fit power-law model, when N_H was fixed to 6.7 $\times 10^{20}$ cm^{-2}, as found for $ROSAT$ PSPC spectrum. (b) The $ASCA$ GIS-3 and $ROSAT$ PSPC spectra of X1832−330, fitted simultaneously using a power law model (α=1.84±0.02) modified with a partial-covering absorber (N_H=7.6$^{+0.5}_{-0.6} \times 10^{21}$ cm^{-2}, covering fraction 0.60$^{+0.2}_{-0.1}$), also with an interstellar absorption model of $N_H = 8.9^{+0.3}_{-0.4} \times 10^{20}$ cm^{-2}.

In Fig. 2(a), we present the average GIS-3 spectrum of X1832−330 with the best-fit power-law model. The fit is poor, with $\chi^2_\nu = 1.81$; the parameters are photon index $\alpha = 1.75\pm0.01$ and N_H=3.6$^{+0.2}_{-0.1} \times 10^{21}$ cm^{-1}, and a 2–8 keV flux of 1.54×10^{-10} ergs cm^{-2}s^{-1}. Note that the fitted N_H is considerably greater than that estimated from the optical extinction ($\sim 5 \times 10^{20}$ cm^{-2}) or the value derived from the $ROSAT$ PSPC spectral fit (6.7$\pm$0.2 × 10^{20} cm^{-2}; see also the bottom panel of Fig. 2(a)). Moreover, the inferred photon index α is radically different between the $ASCA$ GIS (1.75) and $ROSAT$ PSPC (1.07) observations. We therefore must conclude that the spectrum of X1832−330 is highly variable, more complex than a simple power law, or both.

As a likely candidate for the complex spectral shape, we have tried a power law modified by a partial covering absorber (with a fixed interstellar absorption of $\sim 5 \times 10^{20}$ cm^{-2}) to the GIS-3 data. This has markedly improved the fit (to χ^2_ν=1.15; α=1.86$^{+0.03}_{-0.02}$, with $\sim$67% covering by a N_H=7.6$\pm$0.9 × 10^{21} cm^{-2} absorber). Moreover, this model provides a plausible description of the spectrum in a simultaneous fit to the $ASCA$ GIS and $ROSAT$ PSPC spectra (Fig. 2(b)). We therefore conclude that the X-ray spectrum of X1832−330 is not a simple power law. However, given the energy range of the data, and the current level of calibration uncertainties, we cannot say for sure if this description of the spectral shape is unique, or preferred.

In Table 1, we have summarized the long-term history of the X-ray luminosity of X1832−330.

3.2. SIS Data

For the time intervals when both GIS-3 and the SIS instruments were taking data, the latter adds little. However, we have discovered a Type I X-ray burst from X1832−330 in the section of SIS data for which there is no GIS-3 coverage. The light curves in three energy bands are shown in Fig. 3(a). The reason why this burst was not covered by the GIS-3 data is that this happened just before *ASCA* went into the SAA; the high voltage level of the GIS had already been reduced as a precaution. This segment of data ends when the SIS also stopped taking data, as *ASCA* approached the SAA. We have therefore examined the housekeeping as well as scientific data carefully to ascertain that this event is not an instrumental artefact. However, the radiation belt monitor counts indicate that the particle background was <10 ct s^{-1}, i.e., at quiescent (non-SAA) level (all data with monitor rates up to 500 ct s^{-1} have routinely been included in GIS data analysis, with no obvious ill effects). The monitor rate exceeded 1000 ct s^{-1} $\sim$200 s after the end of the SIS data (in contrast, the radiation belt monitor rates exceed 10,000 in the heart of the SAA). Moreover, the image of the burst is identical, to within statistics, to the quiescent image (i.e., has a distribution consistent with the XRT point spread function). Thus, we believe that the burst originates from the same point-like source as the quiescent emission, i.e., most likely X1832−330 in NGC 6652.

The longer duration at lower energies, shown in Fig. 3(a), is what is expected in a Type I X-ray burst, as the neutron star cools. To further investigate the spectral evolution, we have performed spectral fitting of the 4 time intervals indicated in Fig. 3(a). We have used the combined SIS-0/SIS-1 data, and the quiescent SIS spectrum as the background. We present the results of blackbody fits in Fig. 3(b). For interval 1, we find that a significant N_H is required to fit the data adequately; for the other intervals, the fitted N_H values are consistent with the interstellar N_H ($\sim$5$\times10^{20}$ cm^{-2}), once the systematic offset of 1.6×10^{21} cm^{-2} (see §2) has been taken into account.

As is typical of Type I bursts, the color temperature shows a significant decline during the decay of the burst. The inferred radius of the blackbody emitter (we have used the distance of 9.3 kpc and included the normalization correction factor of 1.17) also shows behavior typical of Type I bursts,

Table 1. Long-term Variability of X1832−330.

Epoch	Instrument	2–8 keV Flux[a]	2–8 keV Luminosity[b]
1977/1978	*HEAO-1* A1[c]	8.3 $\times10^{-12}$	8.6 $\times10^{34}$
1992 Apr	*ROSAT* PSPC	1.16 $\times10^{-10}$	1.2 $\times10^{36}$
1996 Apr	*ASCA* GIS	1.54 $\times10^{-10}$	1.6 $\times10^{36}$
1996 & 1997	*BeppoSAX* WFC	5.4 $\times10^{-11}$	5.6 $\times10^{35}$

[a]Measured or inferred flux in the 2–8 keV band, in ergs cm^{-2}s^{-1}.
[b]Inferred 2–8 keV luminosity in erg s^{-1} for an assumed distance of 9.3 kpc.
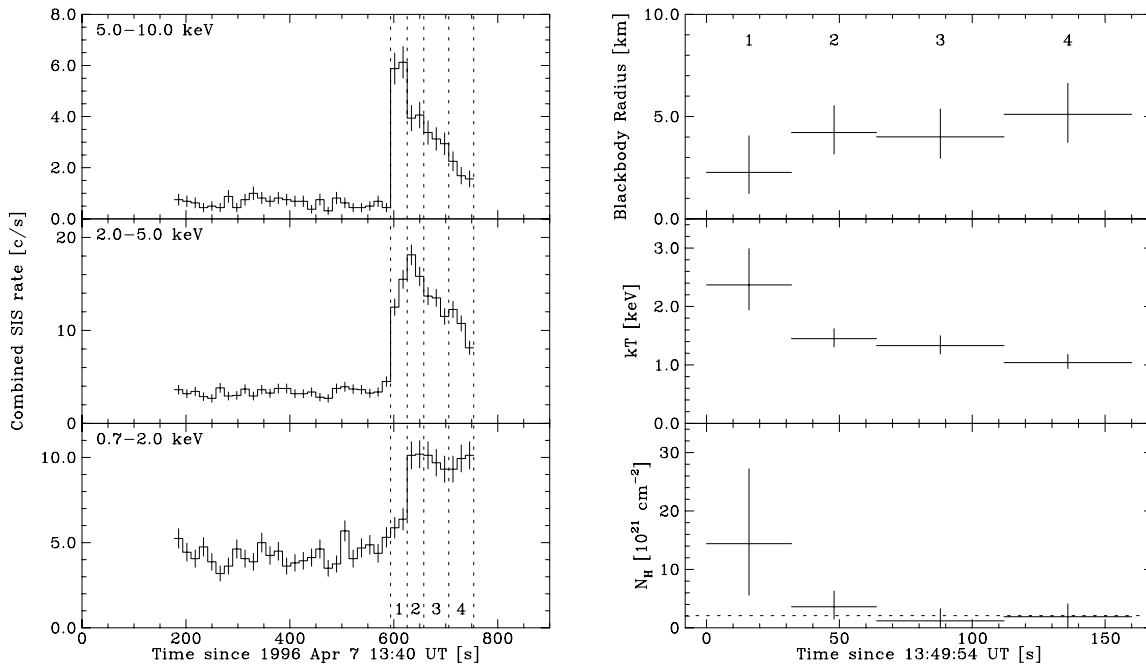[c]Source identification remains tentative.

Fig. 3.— (a) The SIS light curve of the X-ray burst, in 3 energy bins. Time intervals used for the spectral fitting are also indicated. (b) The results of the burst spectral fits.

although it may be on the small side. The inferred bolometric flux during interval 1 is 2.03×10^{-9} ergs cm^{-2}s^{-1}, thus the bolometric luminosity is 2.1×10^{37} ergs s^{-1}. This may underestimate the true peak flux/luminosity somewhat, due to the limited time resolution of our data; judging by the light curve, the true peak values are unlikely to be greater by >1.5 compared with the interval 1 averages. The burst fluence (integrated over the 160s interval for which we have data) is estimated to be 1.45×10^{-7} ergs cm^{-2} (equivalently, total burst energy of 1.45×10^{39} ergs); the fact that we did not see the return to quiescence may have resulted in underestimating this by $\sim10\%$. Thus the average duration τ of the burst was ~71 s.

4. Discussion

The quiescent X-ray spectrum of X1832−330 appears to have a complex shape. A pointed X-ray observation of X1832−330 with a wide spectral coverage appears worthwhile: If the complex shape is indeed due to a partial covering absorber, we then need to understand where it could be located, particularly if X1832−330 is a low inclination system.

We have observed a Type I X-ray burst; although this is not the first from this system to be reported (in't Zand et al 1998), ours is the first time-resolved spectral analysis of a burst from

X1832−330. The spectral cooling we observe is typical of Type I bursts, and can be considered the definitive evidence that X1832−330 is a neutron star binary. The burst appeared to have peaked at around ∼10% Eddington luminosity, but with a typical total fluence. We have approximately 160 s of data after the onset of the burst, and X1832−330 clearly had not completed its return to the quiescent state by the end of this data segment; the duration τ was about 70 s. While this duration is relatively long among all X-ray bursts, it is actually typical of systems with low persistent luminosities (γ, the ratio of persistent flux to Eddington luminosity, is about is about 1% for X1832−330): τ ranges from 30s to a few minutes at $\log \gamma \sim -2$ (van Paradijs et al 1988). We conclude that the *ASCA* burst was a typical Type I event.

Deutsch et al (1998) have recently suggested a relatively faint star, star 49, as a possible optical counterpart. This faintness may be intrinsic, or geometric: since most of the optical light from an LMXB is due to reprocessing in the ∼flat accretion disk, a high binary inclination can lead to an apparently faint optical counterpart. We can comment on this possibility, as the GIS-3 light curve probably is the most suitable X-ray data for orbital period search ever obtained for X1832−330. Since we do not detect orbital modulations, such as eclipses, dips, or quasi-sinusoidal modulations, we conclude that X1832−330 is unlikely to be a high inclination system.

X1832−330 was seen at X-ray luminosity levels ($\sim 10^{36}$ ergs s^{-1}) typical of X-ray bursters during the *ROSAT* and *ASCA* observations. This lends additional support against X1832−330 being a high-inclination, Accretion Disc Corona source. Moreover, we (as well as in't Zand et al (1998)) observed what appears to be a typical Type I X-ray burst, suggesting that we do directly observe the neutron star in X1832−330. These provide additional arguments against X1832−330 being a high inclination system.

If this LMXB is at a low inclination, then a natural explanation for the optical faintness would be that it is ultra-compact, perhaps similar to X1820−303 in NGC 6624 (Anderson et al 1997). Since optical luminosity is dominated by reprocessing, smaller systems tend to be optically fainter. We consider this to be a circumstantial evidence for X1832−330 being an ultracompact binary, joining those in NGC 6624, NGC 6712, and perhaps NGC 1851 (Stella et al 1987; Homer et al 1996; Deutsch et al 1996).

REFERENCES

Anderson, S.F., Margon, B., Deutsch, E.W., Downes, R.A. & Allen, R.G. 1997, ApJ, 482, L69.

Chaboyer, B., Demarque, P. & Sarajedini, A. 1996, ApJ, 459, 558.

Deutsch, E.W., Anderson, S.A., Margon, B. & Downes, R.A. 1996, ApJ, 472, L97.

Deutsch, E.W., Margon, B. & Anderson, S.A. 1998, AJ, 116, 1301.

Dotani, T., Yamashita, A., Rasmussen, A. & the SIS team 1995, *ASCANews* 3, 25.

Hertz, P. & Wood, K.S. 1985, ApJ, 290, 171.

Homer, L., Charles, P.A., Naylor, T., van Paradijs, J., Aurier, M. & Koch-Miramond, L. 1996, MNRAS, 282, 37.

in't Zand, J.J.M., Verbunt, F., Heise, J., Muller, J.M., Bazzano, A., Cocchi, M., Natalucci, L. & Ubertini, P. 1998, A&A, 329, L37.

Johnston, H.M., Verbunt, F. & Hasinger, G. 1996, A&A, 309, 116.

Ortolani, S., Bica, E. & Barbuy, B. 1994, A&A, 286, 444.

Predehl, P., Hasinger, G. & Verbunt, F. 1991, A&A, 246, L21.

Stella, L., White, N.E. & Priedhorsky, W. 1987, ApJ, 312, L17.

Tanaka, Y., Inoue, H. & Holt, S.S. 1994, PASJ, 46, L37.

van Paradijs, J., Pennix, W. & Lewin, W.H.G. 1988, MNRAS, 233, 437.

van Paradijs, J. 1995, in *X-ray Binaries*, ed. W.H.G. Lewin, J.van Paradijs & E.P.J. van den Heuvel (Cambridge: Cambridge Univ. Press), 536.